



University  
of Glasgow

Viavattene, G. and Ceriotti, M. (2021) Low-thrust multiple asteroid missions with return to earth using machine learning. In: 2020 AAS/AIAA Astrodynamics Specialist Conference, 9-12 August 2020, AAS 20-645. ISBN 9780877036753

This is the Author Accepted Manuscript.

There may be differences between this version and the published version. You are advised to consult the publisher's version if you wish to cite from it.

<http://eprints.gla.ac.uk/222201/>

Deposited on: 14 August 2020

Enlighten – Research publications by members of the University of Glasgow  
<http://eprints.gla.ac.uk>

# LOW-THRUST MULTIPLE ASTEROID MISSIONS WITH RETURN TO EARTH USING MACHINE LEARNING

Giulia Viavattene\*, Matteo Ceriotti†

Sample-return missions to near-Earth asteroids (NEAs) are invaluable for the scientific community to learn more about the initial stages of the solar system formation and life evolution. Thanks to its high specific impulse, a low-thrust propulsion technology is capable of performing multiple asteroid rendezvous (to collect samples) and eventually returning to Earth. To identify the best asteroid sequences with return to Earth, this work proposes to employ machine learning techniques and, specifically, artificial neural networks (ANNs), to quickly estimate the cost of each transfer between asteroids. The ANN is integrated within a sequence search algorithm based on a tree search, which identifies the asteroid sequences and selects the best ones in terms of propellant mass required and interest value. This algorithm can design the sequences so that specific asteroids of interest, for which a sample return would be more valuable, can be targeted. A pseudospectral optimal control solver is then used to find the optimal trajectory and control history. The performance of the proposed methodology is assessed by analyzing three distinctive NEA sequences ending with return to Earth and rendezvous. A near-term low-thrust propulsion enables to rendezvous five asteroids, and ideally return samples to Earth in about ten years from launch. It is demonstrated that visiting more interesting asteroids from the scientific point of view increases the appeal of the sequence at the cost of a greater propellant mass required.

## INTRODUCTION

The first sample return missions, which have been completed, are the Apollo Moon mission and Russian Luna 16, 20 and 24 missions launched between 1968 and 1976, which returned successfully samples of the lunar surface to the Earth. This contributed greatly to understand Moon's geological history and composition.<sup>1</sup> Similarly, the scientific community is interested in collecting samples from the surface of asteroids. Because of the lack of ground observations or quality data the asteroids' composition is largely unknown and, as it is anticipated to vary considerably from asteroid to asteroid, collecting samples from multiple asteroids is valuable. It is expected that this will allow to learn more about the initial stages of the solar system formation and how life began.<sup>2,3</sup> Additional motivations that drive scientists to further study asteroids and, in particular, near-Earth asteroids (NEAs) are planetary defense,<sup>4</sup> scientific demonstration<sup>5,6</sup> and future exploitation of their resources.<sup>7</sup>

To date, the JAXA Hayabusa probe rendezvoused with an S-type asteroid 25143 Itokawa and, in November 2010, it returned an asteroid sample to Earth.<sup>8</sup> In 2014 JAXA launched the improved Hayabusa 2 probe to visit a near-Earth C-type asteroid 162173 Ryugu. It took samples of the

\*James Watt School of Engineering, University of Glasgow, Glasgow G12 8QQ, United Kingdom, g.viavattene.1@research.gla.ac.uk.

†James Watt School of Engineering, University of Glasgow, Glasgow G12 8QQ, United Kingdom.

asteroid surface and it is expected to return to Earth in late 2020.<sup>9</sup> The OSIRIS-REx mission was launched by NASA in 2016 to return samples from the near-Earth asteroid 101955 Bennu.<sup>2</sup>

Return missions of planetary and small-body samples represent one of the biggest challenges for the space engineering. The  $\Delta V$  required to complete this kind of missions can greatly outrun the one necessary to fly one-way missions and, according to the rocket equation, with increasing  $\Delta V$  the propellant mass to complete the mission increases exponentially. Also, a high  $\Delta V$  requires the payload mass fraction to be inevitably small so that more propellant can be carried on board, which consequently limits the dry mass and the maximum mass of samples which can be returned to Earth.<sup>10</sup>

Rendezvousing multiple NEAs with sample return to Earth can increase the scientific return of those missions.<sup>11,12</sup> Multiple-NEA missions give the possibility of visiting a larger number of asteroids, from which samples can be extracted and returned to Earth for further studies. This kind of missions can thus reduce the cost with respect to performing multiple space flights to a single asteroid and relative sample return.

Multiple-target rendezvous missions are highly demanding in terms of energy, and they are even more so when followed by a sample return to Earth. For this reason, an efficient propulsion system is required to significantly keep the propellant mass ratio low. Low-thrust technologies, such as solar electric propulsion (SEP), are a good candidate because of its high specific impulse.<sup>13,14</sup>

To design multiple NEA rendezvous missions, a complex global optimization problem needs to be solved. This is constituted by two coupled sub-problems.<sup>15</sup> The first is a large combinatorial sub-problem, which encodes the selection of the sequences of asteroids.<sup>16</sup> To this end, trillions of permutations should be analyzed, since more than 22,000 asteroids are known to date, according to NASA's database\*. The second sub-problem is continuous, and consists in finding the solution to an optimal control problem (OCP) to obtain the optimal flight trajectory to visit the selected asteroids with minimum propellant expenditure and/or time of flight (TOF). It should be stressed that the two problems cannot be solved independently from each other, as the combinatorial part requires inputs, such as duration and cost of each transfer, which are obtained by solving the continuous sub-problem, and viceversa. This study proposes to use machine learning to solve the combinatorial problem and, at the same time, the continuous problem through estimates.

The design of multiple asteroid missions has interested the space community in the past decades. Asteroid-related problems were proposed in six out of the eight Global Trajectory Optimization Competitions (GTOC)<sup>†</sup>. The majority of the proposed solutions suggests to use a simplified trajectory model to obtain the asteroid sequence and, more accurate and complex methods to convert the obtained sequence into a feasible low-thrust trajectory. For instance, in Piloni et al. (2016),<sup>17</sup> low-thrust trajectories are approximated using a shape-based method and a search-and-prune algorithm is used to find the sequence. Differently, a homotopic approach is used in Tang et al. (2015),<sup>18</sup> to quickly approximate the low-thrust transfers. Di Carlo et al. (2017)<sup>19</sup> proposes to traverse the asteroid belt with a high elliptical orbit and visit as many asteroids as possible that are encountered along that orbit.

In the past, machine learning was applied successfully to solve complex problems in aerospace

---

\*Data available through the link <https://cneos.jpl.nasa.gov/orbits/elements.html> (accessed on 2020/01/10)

<sup>†</sup>Data available through the link [https://sophia.estec.esa.int/gtoc\\_portal/](https://sophia.estec.esa.int/gtoc_portal/) (accessed on 2020/01/10)

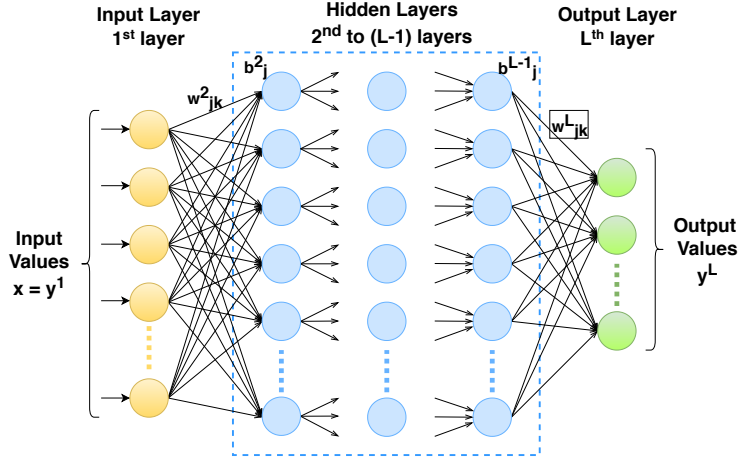


**Figure 1:** Illustration of an ANN with  $L$  layers.

sciences. Dachwald (2004)<sup>20</sup> used artificial neural networks and evolutionary algorithms to compute the solar-sail trajectories to a NEA, showing that this method can explore the trajectory space search more exhaustively than traditional optimal control methods. Similarly, Hennes et al. (2016)<sup>21</sup> used machine learning to compute low-thrust transfers with minimum fuel mass between main-belt asteroids. Mereta et al. (2017)<sup>22</sup> employed machine learning techniques to estimate the final mass of a spacecraft flying a low-thrust trajectory between two NEAs, instead of solving the full OCP. Other applications include the increase of accuracy of pinpoint landing<sup>23</sup> and orbit prediction,<sup>24</sup> and the design of multiple NEA missions using solar sailing<sup>25</sup> or solar electric propulsion.<sup>26</sup>

The purpose of this work is to use an Artificial Neural Network (ANN) to identify the most effective sequences of asteroids to visit and then return to Earth. It will be shown that a trained ANN can *quickly* estimate, in a fraction of the time needed by optimal control solvers, the cost and TOF of transfers using a near-term low-thrust propulsion system, vastly reducing the computational time compared to traditional optimization techniques.<sup>26</sup> The ANN is integrated within a sequence search algorithm which allows the spacecraft to return to Earth within the maximum duration of the mission.

## MACHINE LEARNING FOR LOW-THRUST TRANSFERS

Inspired by the biological cognitive systems of the animal brain, an ANN is a complex computing system that can model complex non-linear relationship to any degree of accuracy.<sup>27</sup> For function approximation, feedforward networks are preferred.<sup>28</sup> A neural network is organized in layers and information moves from the *input layer* to the *output layer* through a number of *hidden layers*. Each layer presents a defined amount of neurons and each neuron is connected directly to the neurons of the successive layer,<sup>29</sup> as shown in Fig. 1.

The network is trained so that the mean-squared error between the network outputs  $y$  and targets  $y_t$  is minimized:

$$\mathcal{E}_{MSE} = \frac{1}{N} \sum_{i=1}^N |y_i - y_{t,i}|^2 \quad (1)$$

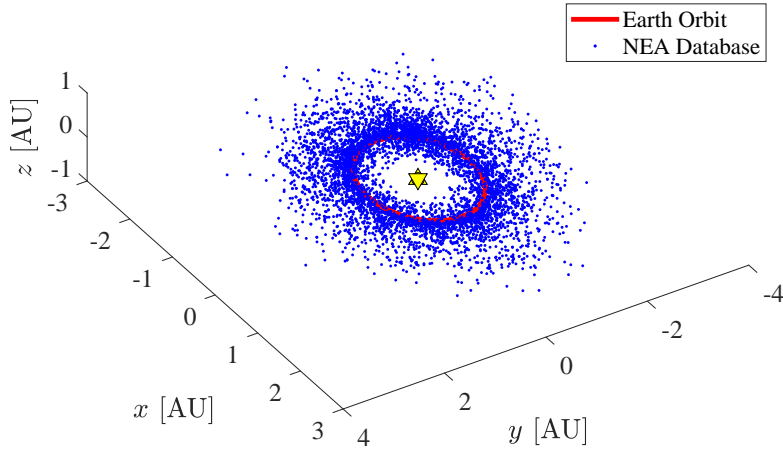


**Figure 2:** NEAs selected for the generation of the training database.

with  $N$  being the number of outputs. Also, to ensure that the outputs fit well the targets, the correlation between the network outputs and targets is maximized, i.e., as close as possible to unity.

Designing a neural network for a particular application presents different challenges. Firstly, the identification of a method to generate the training database. Secondly, since the topology and hyper-parameters of the network influence the network accuracy, the values for each of these parameters, which offer the best network performance, need to be identified. These points are addressed in the next two sections.

### Training Database Generation

The training database contains the input vector and the target output vector. The input vector includes the orbital parametrization of the departure and arrival asteroids and the position along their orbits at a reference time. The target output vector includes the cost  $\Delta V$  and TOF of the low-thrust, rendezvous transfers between the departure and arrival asteroids. It follows that the input vector  $\mathbf{x}$  and output vector  $\mathbf{y}$  can be defined as:

$$\mathbf{x} = [p_0, f_0, g_0, h_0, k_0, L_0, p_f, f_f, g_f, h_f, k_f, L_f] \quad (2)$$

$$\mathbf{y} = [\Delta V, t_{0,f}] \quad (3)$$

where  $p_0, f_0, g_0, h_0, k_0, L_0$  and  $p_f, f_f, g_f, h_f, k_f, L_f$  are the modified equinoctial elements (MEE)<sup>30</sup> describing, respectively, the orbits of the departure and arrival NEAs,  $\Delta V$  indicates the velocity increment and  $t_{0,f}$  the time of flight.

For the generation of the database, NEAs which are of particular scientific interest, composition and/or orbit are included, such as Potentially Hazardous Asteroids (PHA) and Near-Earth Object Human Space Flight Accessible Targets Study (NHATS). Figure 2 shows the 6,286 NEAs, which are used for the simulation, at their position (blue dots) with respect to the Earth's orbit (in red) on 27 April 2019. The orbital elements of these NEAs (*input*) are obtained from the NASA's Near-Earth Object Program.\*

\*Data available through the link <https://cneos.jpl.nasa.gov/orbits/elements.html> (accessed on 2019/06/17)

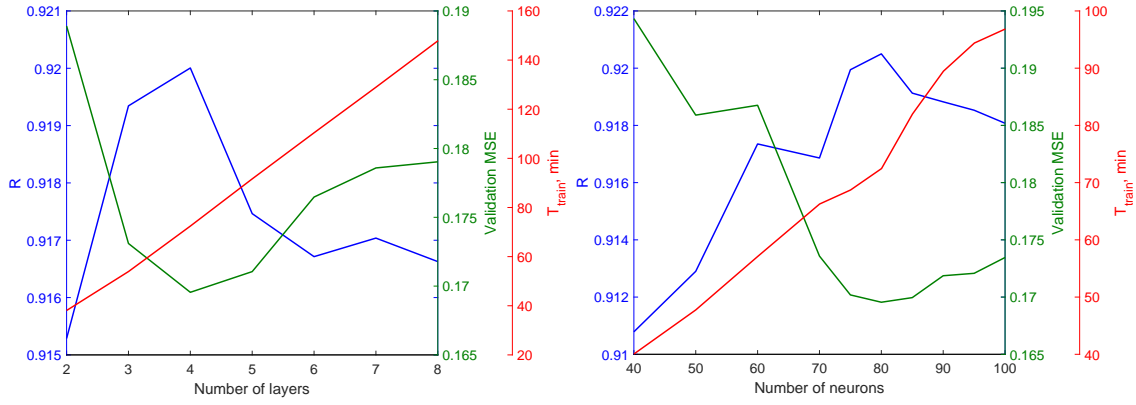


**Figure 3:** Effect of varying the network parameters on the correlation coefficient  $R$ , validation-set MSE and training time.

To compute the  $\Delta V$  and TOF of low-thrust transfers (*output*) between the couples of asteroids, an OCP needs to be solved. Considering that a sufficient number of samples is needed to accurately train the network, direct or indirect methods are excluded as they require a long computation time. Analytical methods can, instead, provide a quick and reliable, but approximated, trajectory description. For this work, the shape-based method<sup>31</sup> is chosen to approximate the shape of low-thrust transfers, for the given launch dates and propulsion system, and to estimate the related  $\Delta V$  and TOF. A genetic algorithm is used to compute the shaping parameters to obtain the rendezvous transfers with minimum cost. From the obtained acceleration profile, the control history can be retrieved.

The training database is build by permuting a subset of 100 NEAs and using the shape-based method to compute the cost and duration of the transfers for each couple of asteroids. All the departures dates are included in a launch window from January 2020 and December 2030. The training database comprises a total of 10,100 low-thrust transfers. The number of NEAs and the launch window are bounded for the generation of the training database. This is done to verify the *generalization* property of the neural network, for which a successfully trained ANN can generalize and estimate transfer costs between NEAs that are not included in the database and with different launch dates.

To verify the generalization property of the network, the database is divided into training set, validation set and test set. The training set is used for the training, while the validation and test sets contain new samples that are not included in the training. The validation set is used to verify that the overfitting does not occur during the training and the test set is used to test the performance of the network, after the training, with totally new cases. To this end, the validation-set MSE is often taken into consideration when studying the network performance.

### Network Architecture Design

The architecture of the network is defined by the number of hidden layers and the number of neurons. Other hyper-parameters of the network are the learning algorithm, activation function for each hidden layer, learning rate or gradient constant and its increase or decrease factor. Also, different orbit parametrizations can be used as inputs to the network, showing that the choice of the right type of inputs can influence the performance of the network.

**Table 1:** Network architecture and hyper-parameters for the highest network performance.

ANN Parameter	Best value
Number of hidden layers	4
Number of neurons of each hidden layers	80
Learning algorithm	Levenberg-Marquardt
Activation function of each hidden layers	sigmoid
Gradient Constant $\mu$	0.001
Decrease Factor $\mu_{dec}$	01
Database division rates (training:validation:test)	70:15:15
Orbit parametrization for the network inputs	MEE

The effect of varying the hyper-parameters and the input of the network on its performance is studied with the purpose of identifying the combinations of parameter values that offer the highest network performance. Figure 3 shows the response of the network to varying the number of layers and neurons on the correlation coefficient  $R$ , MSE of the validation set and training time  $T_{train}$ . While the training time increases significantly as the number of layers and/or neurons increases, the performance of the network reaches a peak for a specific number of hidden layers and neurons.

A similar analysis is performed for each of the other network hyper-parameters and different orbit parametrizations used as the network input. The interested reader can find the detailed description of these analyses in the other paper from the authors.<sup>26</sup> Table 1 presents the parameters of the network which led to the highest performance for the cost estimation of low-thrust transfers, with final correlation coefficient of 0.9732 and validation-set MSE of 0.1211.

## SEQUENCE SEARCH ALGORITHM

The following sequence search algorithm is implemented to identify the most promising sequences of asteroids to visit with the final return to Earth. The logic of the algorithm is based on a *tree-search* method and it is schematized in Figure 4. The search starts from Earth as the departure body at a fixed launch date. The NEA database is loaded and their ephemerides are updated at the departure date  $t_{0,i}$ , where  $i$  indicates the  $i$ -th leg. The ANN is embedded within this algorithm to compute the cost and duration of low-thrust, rendezvous transfers from Earth to all the NEAs in the database. The  $N_S = 200$  trajectories with the least propellant mass required are stored and a stay time  $t_{stay} = 100$  days is added at each object to ensure enough time for close-up observation and/or sample collection. At this point, the arrival body becomes the departure body of the following leg and the same procedure is iterated. If the total mission duration is longer than six years, a pruning of the asteroids to be considered in the search is performed to guarantee that the spacecraft can successfully return to Earth on its last leg. To this end, the algorithm is designed to select the next body among those NEAs whose semimajor axis, eccentricity and inclination are included between the last NEA visited in the sequence and the Earth, i.e.:

$$a_n \leq a \leq a_E \quad (4)$$

$$e_n \leq e \leq e_E \quad (5)$$

$$i_n \leq i \leq i_E \quad (6)$$

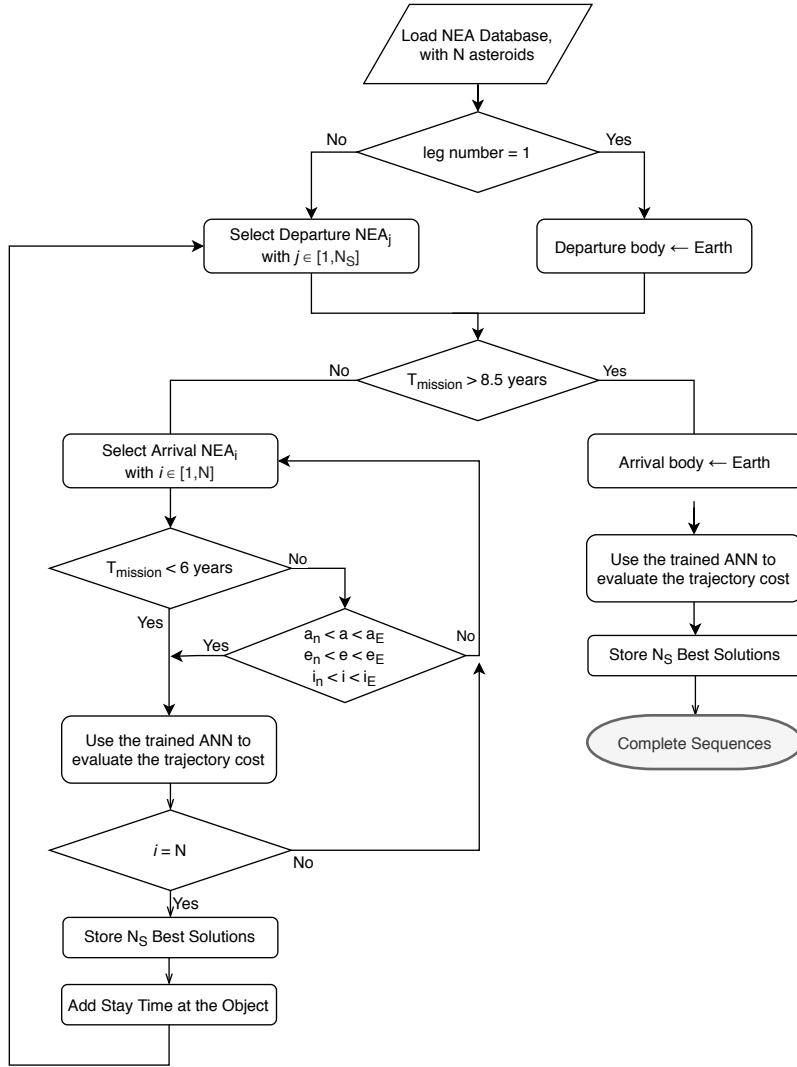


**Figure 4:** Sequence search algorithm with return to Earth.

where  $n$  indicates the  $n$ -th asteroid visited and  $E$  the Earth. In essence, this induces the search to target asteroids that are incrementally more similar to Earth in terms of orbital elements. The expressions are defined for the case with  $a_E \geq a_n$ ,  $e_E \geq e_n$ , and  $i_E \geq i_n$ , but they are inverted when the opposite case is verified.

When the mission duration exceeds 8.5 years, it is expected that the spacecraft will orbit close enough to Earth that the final return leg can be performed. The ANN is also used in this case to estimate the trajectory cost. Finally, the best solutions in terms of propellant mass expenditure are stored and considered as complete sequences.

Figure 5 shows the sequences with five asteroids visited and return to Earth which were calculated by the sequence search algorithm for the departure date 24 August 2035. Since the number of asteroids to visit grows rapidly as we proceed through the legs, only the first three legs are plotted in full and, for illustration, one complete sequence is fully shown.



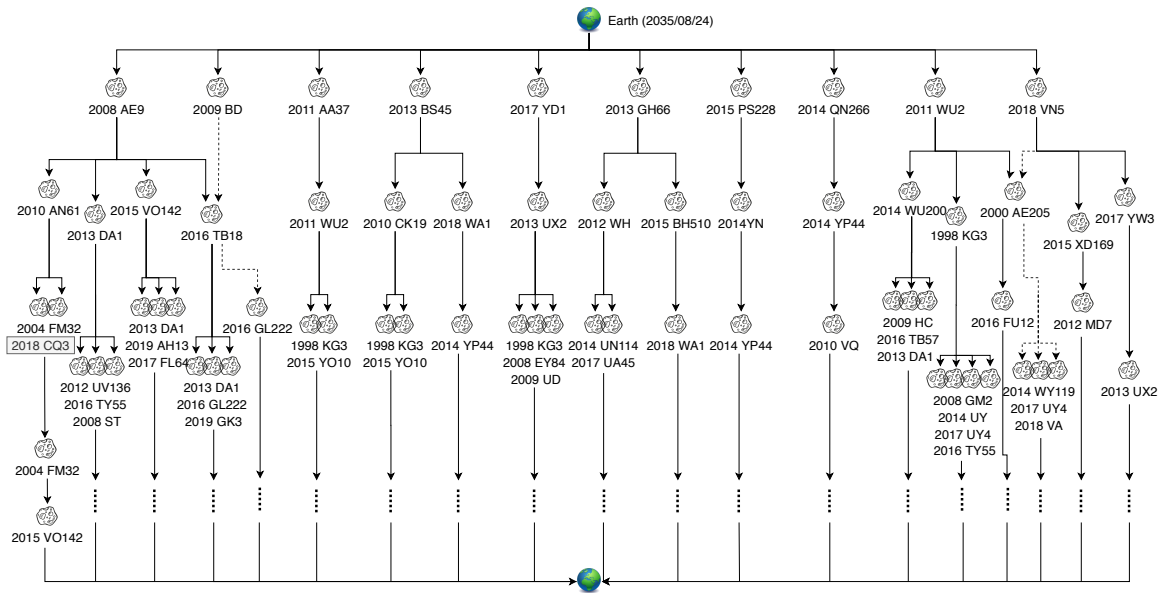


**Figure 5:** Tree graph of first three legs of the sequences visiting five asteroids and returning to Earth, which were found for launch date 24 August 2035.

## Asteroid Targeting

As mentioned in the introduction, the previous missions, which performed to date a successful sample return to Earth, were designed to target one asteroid which is reachable with the given propulsion system and particularly interesting from the scientific point view. For instance, 25143 Itokawa and 162173 Ryugu were selected as the target asteroids for the missions Hayabusa and Hayabusa 2, respectively, because they are suitable target in terms of asteroid size and are reachable using an ion engine with a realistic  $\Delta V$ .<sup>8,9</sup> Similarly, NASA selected the asteroid 101955 Bennu for the mission OSIRIS-REx as it is rich in pristine carbonaceous material, which is a key element in organic molecules necessary for life.<sup>2</sup> In all the three missions, the asteroids were chosen primarily because the sample collections and analyses are expected to improve the knowledge on the formation and evolution of the planets and, in particular, of Earth, as well as the origin of water and organic matter.

The sequence search algorithm can be adjusted to target a specific asteroid that is particularly interesting for the scientific community and for which a sample return would be more valuable. Figure 6 schematizes the sequence search algorithm which is implemented to target one asteroid within the sequence and finally return to Earth. Compared to the previous algorithm with no NEA targeting, this algorithm works so that the first half of the sequence is focused on targeting the chosen asteroid of interest, while the second half is focused on targeting the Earth for a safe reentry.

The purpose is to ensure that the spacecraft can reach the target asteroid and, simultaneously, visit as many asteroids as possible for observations and/or sample collections, while the spacecraft flies from Earth to the target body and back to Earth. To this end, a pruning of the asteroids that are visited between the departure from Earth and the arrival at the target body is also performed. Only the NEAs with semimajor axis, eccentricity and inclination included between those of Earth and the target asteroid are considered, i.e.:

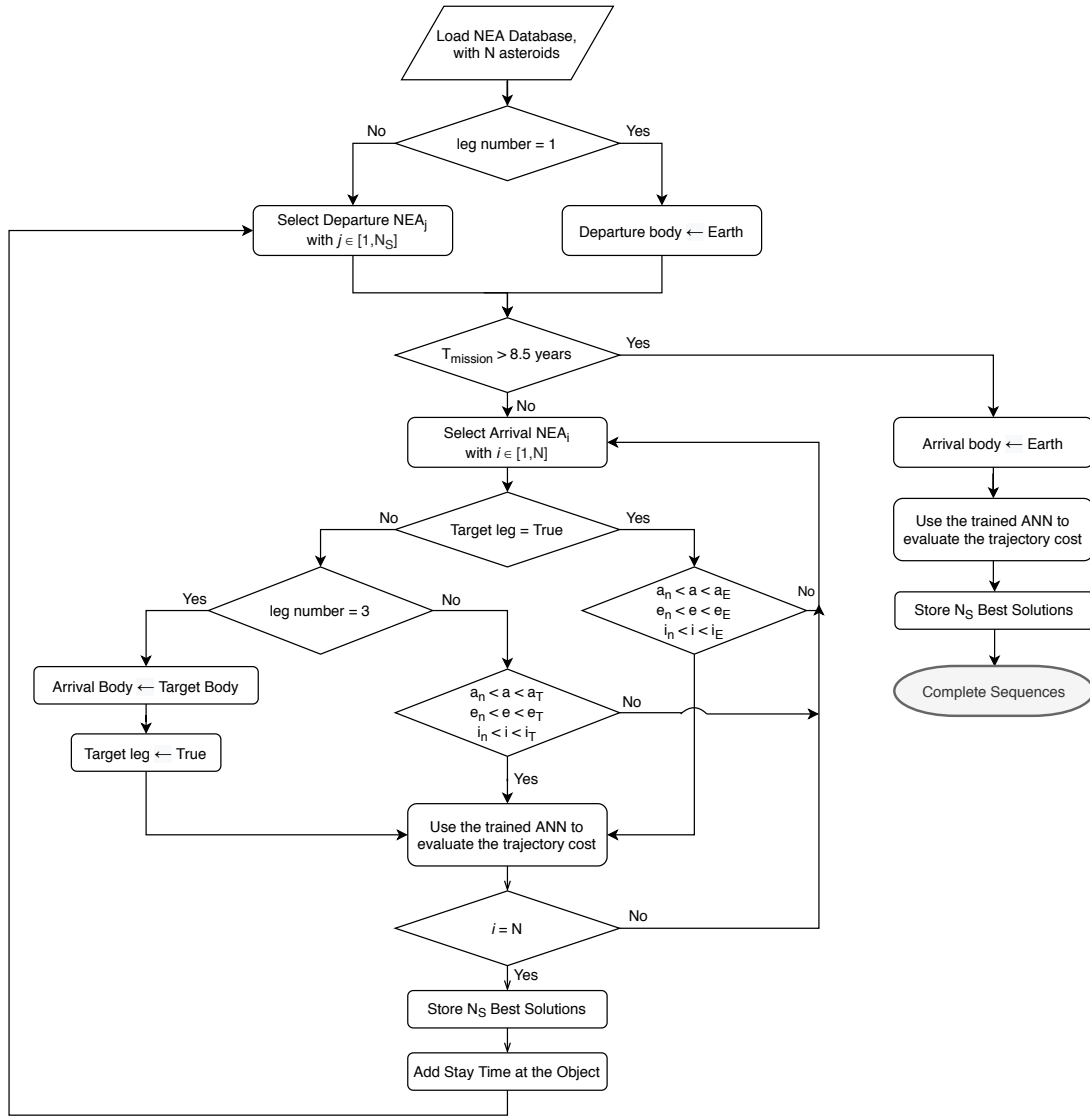


**Figure 6:** Sequence search algorithm to target one NEA of interest and return to Earth.

$$a_n \leq a \leq a_T \quad (7)$$

$$e_n \leq e \leq e_T \quad (8)$$

$$i_n \leq i \leq i_T \quad (9)$$

where  $n$  indicates the  $n$ -th asteroid visited (or Earth for the first leg) and  $T$  the targeted asteroid. After two legs have been performed, it is assumed that the spacecraft has reached an orbit from which it is possible to conveniently, in terms of cost and duration of the transfer, reach the target body. Thus, the arrival body of the third leg is the target asteroid.

Once the target body is visited and the sample is collected, a second pruning of the asteroids, which are visited between the departure from the target body and the return to Earth, is performed.

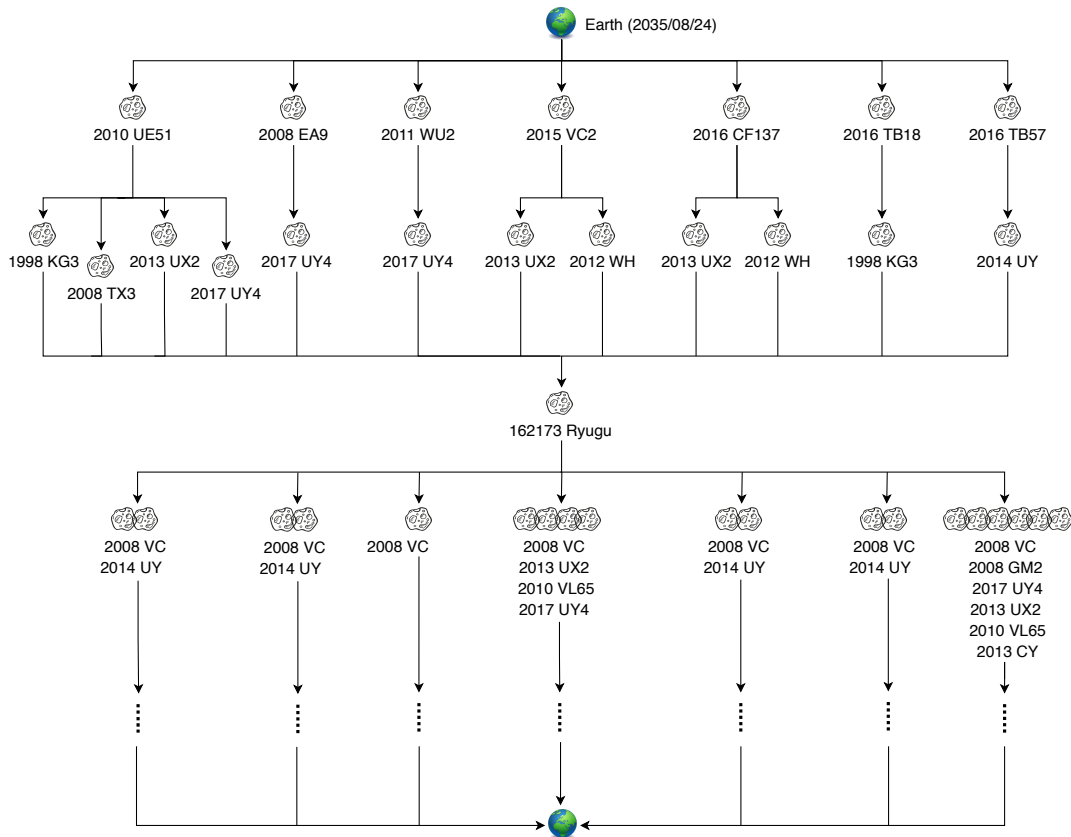


**Figure 7:** Tree graph of the sequences targeting 162173 Ryugu in the third leg and visiting five asteroids before returning to Earth. These sequences are obtained for the launch date 24 August 2035.

This is done, similarly to the previous algorithm represented in Figure 4, to guarantee that the spacecraft can successfully return to Earth and visit as many asteroids as possible in its way back to Earth.

For this work, the asteroid 162173 Ryugu is targeted, which is a PHA and NHATS of the Apollo group with approximately 1 km in diameter. This asteroid was previously chosen by JAXA as it has an unaltered or barely altered composition (C-type) and it is easily accessible from Earth.<sup>32</sup> Figure 7 shows the tree graph of the sequences of five asteroids, which target 162173 Ryugu in the third leg and, finally, return to Earth. These sequences are calculated by the sequence search algorithm for the departure date 24 August 2035.

### Interest Value of NEA Sequences

As many asteroids remain *unclassified* due to the lack of quality data or limited opportunities for ground observation,<sup>33</sup> it is chosen to consider more valuable to observe, collect and return samples of NEAs, which are bigger in size, so that they can be classified. Larger asteroids are generally rarer and more suitable for landing and for the sample collection.

Apart from the asteroids which have been visited by a spacecraft in the past, the size and shape of most asteroids is yet unknown. Although most asteroids have irregular shape and only few of them

are close to being spherical, the size of an asteroid can be estimated from its *absolute magnitude*,  $H$ , and assumed geometric albedo,  $a$ , as the diameter of an equivalent sphere with a uniform surface. The diameter (in km) of an asteroid can be estimated as follows:<sup>34</sup>

$$d = 10^{(3.1236 - 0.5 \log_{10}(a) - 0.2H)} \quad [km] \quad (10)$$

where the albedo,  $a$ , is generally assumed based on the spectral class corresponding to the assumed composition of the asteroid and an average value is typically used.<sup>35</sup> Due to the conceivable uncertainty in both  $H$  and  $a$ , Eq. (10) provides an approximate estimation of the size of an asteroid. For example, for the same absolute magnitude  $H$ , a deviation in albedo of 0.1 leads to an error in diameter by a factor of two.\* However, considering that in Eq.(10)  $H$  has a larger impact than  $a$  in determining the asteroid's size, we will assume in the following that an asteroid with a smaller  $H$  is characterized by a larger size and, in principle, represents a more interesting candidate to visit in a sequence.

To classify the obtained sequences on the basis of their scientific interest, the *interest value*,  $I_V$ , of each sequence is used and defined as the negative sum of the absolute magnitudes of all the visited asteroids, i.e.:

$$I_V = - \sum_{i=1}^{N_A} H_i \quad (11)$$

where  $H_i$  is the absolute magnitude of the  $i$ -th asteroid visited and  $i \in [1, N_A]$ , with  $N_A$  being the number of asteroids visited during the relative sequence. The greater the interest value, the larger the asteroids visited and the more interesting is considered the sequence.

To take into account the interest value for the selection, during the sequence search, of the most convenient sequences to fly, an *appealing factor*  $A$  is associated to each sequence as the weighted sum of its total  $\Delta V$  and total  $I_V$ , which can be expressed as follows:

$$A = \alpha \Delta V_{n,tot} - (1 - \alpha) I_{V,n,tot} \quad (12)$$

where  $\alpha$  is a weight coefficient, which can vary from 0 to 1 depending on the importance given to the  $\Delta V$  and  $I_V$  when selecting the sequences. Note that  $\Delta V_{n,tot}$  and  $I_{V,n,tot}$  refer to the normalized values of the total  $\Delta V$  and  $I_V$  of the sequence. In this case, the sequence search algorithms are changed so that, at each leg, the  $N_S = 200$  trajectories with the lowest  $A$  are selected, which means minimum  $\Delta V$  and maximum interest value.

Varying the value of the weight  $\alpha$  and/or targeting one asteroid of interest within a sequence have an impact on the final mass expenditure and interest value of the sequence. Figures 8(a) and 8(b) show the distribution of the  $\Delta V$  for all the transfers and  $\Delta V_{tot}$  for all the sequences. Similarly, Figures 8(c) and 8(d) describe the distribution of the absolute magnitude,  $H$ , for all encountered NEAs and interest value,  $I_V$ , for all the sequences. These distributions are obtained when the sequence search algorithm is run for the following cases:

---

\*Data available through the NASA JPL Asteroid Size Estimator [https://cneos.jpl.nasa.gov/tools/ast\\_size\\_est.html](https://cneos.jpl.nasa.gov/tools/ast_size_est.html) (accessed on 2020/07/14)

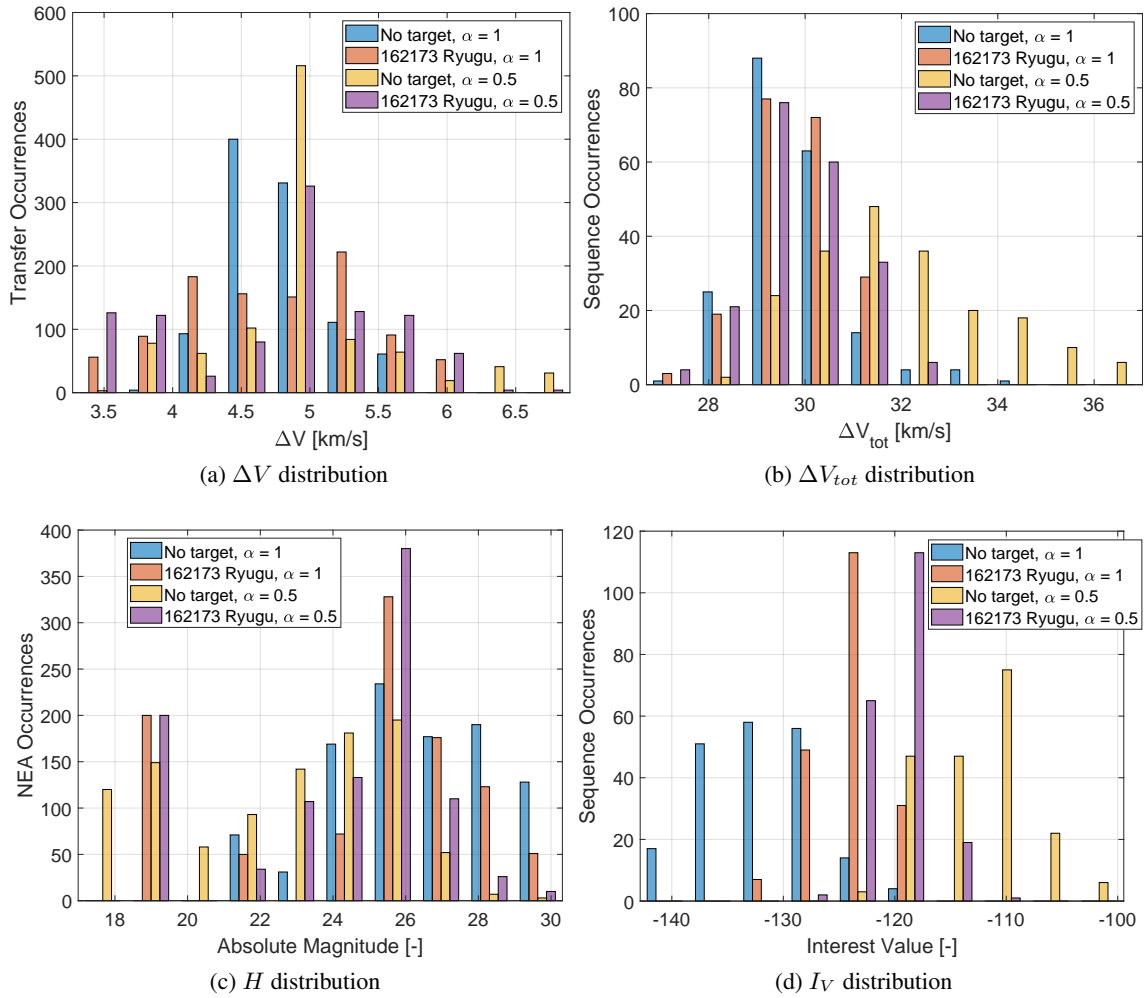


**Figure 8:** Distribution of the  $\Delta V$  (a),  $\Delta V_{tot}$  (b), absolute magnitude  $H$  (c) and interest value  $I_V$  (d) of the obtained sequences and NEAs visited.

1. no target asteroid and  $\alpha = 1$
2. 162173 Ryugu as the target asteroid and  $\alpha = 1$
3. no target asteroids and  $\alpha = 0.5$
4. 162173 Ryugu as the target asteroid and  $\alpha = 0.5$

The figures indicate that when  $\alpha$  is lower than one, i.e., the selection of the sequences is also made on the basis of their  $I_V$ , the selected sequences are characterized by a greater  $I_V$  and generally higher  $\Delta V$  with respect to the case when only the  $\Delta V$  is considered (i.e.,  $\alpha = 1$ ). In the latter case of  $\alpha = 1$ , it is possible to achieve a larger number of sequences with greater  $I_V$  when an interesting asteroid is targeted within the sequences. However, it should be noted that, when  $\alpha < 1$ , the pruning of the asteroids, which is performed to ensure that the target asteroid can be conveniently reached, appears to reduce the likelihood to encounter asteroids with a larger size, compared to the case when

**Table 2:** Orbital characteristics of the NEAs visited in Sequence A.

<b>Sequence A</b>	2008 EA9	2010 AN61	2018 CQ3	2004 FM32	2015 VO142
$a$ , AU	1.05	1.16	1.17	1.10	1.08
$e$ , -	0.07	0.13	0.15	0.16	0.13
$i$ , deg	0.44	3.61	4.00	3.76	0.28
$H$ , -	27.7	27.0	25.2	27.1	28.9
Estimated size, m	8-19	11-24	27-60	11-24	4-10
PHA	No	No	No	No	No
NHATS	Yes	Yes	Yes	Yes	Yes
Orbit Class	Apollo	Apollo	Apollo	Apollo	Apollo

no objects are targeted. In summary, more interesting objects can be favored during the sequence selection process, increasing the overall appeal of the sequences generated by the search algorithm at the cost of a larger  $\Delta V$ .

### MULTIPLE NEA SAMPLE RETURN MISSIONS

To verify the outcome of the sequence search algorithm, three sequences are selected and fully optimized for a solar electric propulsion system with maximum thrust  $T_{max} = 0.3$  N, specific impulse  $I_{sp} = 3000$  s, and initial mass  $m_0 = 1500$  kg. The sequences are selected from the following simulations:

1. Sequence A, chosen as the sequence with lowest  $\Delta V$  obtained from the sequence search with no target asteroid and  $\alpha = 1$
2. Sequence B, chosen as the sequence with lowest  $\Delta V$  obtained from the sequence search with 162173 Ryugu as the target asteroid and  $\alpha = 1$
3. Sequence C, chosen as the sequence with greater  $I_V$  obtained from the sequence search with no the target asteroid and  $\alpha = 0.5$

The orbital characteristics of the asteroids visited during the Sequences A, B and C are detailed in Tables 2, 3 and 4, respectively. The sequences visit five asteroids, of which some are PHA and all are NHATS except for 2000 LY27, which is a PHA and presents the lowest absolute magnitude  $H$ . An estimated size of the asteroids is provided and calculated using the conversion formula from the absolute magnitude to the diameter expressed in Eq. (10), taking into account an albedo in the range 0.05–0.25.

The low-thrust OCP is solved to find the high-fidelity trajectories. The dynamics is described by the following set of ordinary differential equations:

$$\dot{\mathbf{x}}(t) = \mathbf{A}(\mathbf{x})\mathbf{a} + \mathbf{b}(\mathbf{x}) \quad (13)$$

where  $\mathbf{x}$  is the state vector of the system, expressed in modified equinoctial elements and adjoined by the spacecraft mass,  $\mathbf{A}(\mathbf{x})$  and  $\mathbf{b}(\mathbf{x})$  are, respectively, the matrix and the vector of the dynamics, as defined in Ref. 36. The acceleration generated by the SEP system  $\mathbf{a}$  can be described as follows:

**Table 3:** Orbital characteristics of the NEAs visited in Sequence B.

Sequence B	2016 TB18	1998 KG3	162173 Ryugu	2014 UY	2008 EA9
$a$ , AU	1.08	1.16	1.19	1.17	1.05
$e$ , -	0.08	0.12	0.19	0.17	0.07
$i$ , deg	1.53	5.51	5.88	3.56	0.44
H, -	24.8	22.1	19.3	25.4	27.7
Estimated size, m	27-60	110-240	870-1000	21-48	8-19
PHA	No	No	Yes	No	No
NHATS	Yes	Yes	Yes	Yes	Yes
Orbit Class	Apollo	Amor	Apollo	Apollo	Apollo

**Table 4:** Orbital characteristics of the NEAs visited in Sequence C.

Sequence C	1998 KG3	162173 Ryugu	2017 UY4	2000 LY27	2001 QC34
$a$ , AU	1.16	1.19	1.19	1.31	1.13
$e$ , -	0.12	0.19	0.16	0.21	0.19
$i$ , deg	5.51	5.88	3.78	9.02	6.24
H, -	22.1	19.3	25.2	17.0	20.1
Estimated size, m	110-240	870-1000	27-60	1100-2400	270-600
PHA	No	Yes	No	Yes	Yes
NHATS	Yes	Yes	Yes	No	Yes
Orbit Class	Amor	Apollo	Apollo	Amor	Apollo

**Table 5:** Mission parameters of the optimized NEA Sequence A. Comparison of optimal results with ANN estimations (in brackets).

Leg	Departure	Arrival	TOF, days	$\Delta V$ , km/s	Stay Time, days
Earth - 2008 EA9	2035/08/24	2037/04/20	605 (545)	5.96 (5.48)	83
2008 EA9 - 2010 AN61	2037/07/12	2038/11/29	505 (560)	4.80 (4.61)	20
2010 AN61 - 2018 CQ3	2038/12/19	2040/08/19	609 (550)	4.47 (4.43)	20
2018 CQ3 - 2004 FM32	2040/09/08	2042/06/08	638 (558)	4.75 (4.63)	100
2004 FM32 - 2015 VO142	2042/09/16	2043/10/05	384 (368)	3.10 (3.61)	54
2015 VO142 - Earth	2043/11/28	2045/03/31	489 (489)	4.01 (4.34)	–

$$\mathbf{a} = \frac{T_{max}}{m} \mathbf{N} \quad (14)$$

where  $T_{max}$  is the maximum thrust that can be generated and  $\mathbf{N}$  is the acceleration direction. As

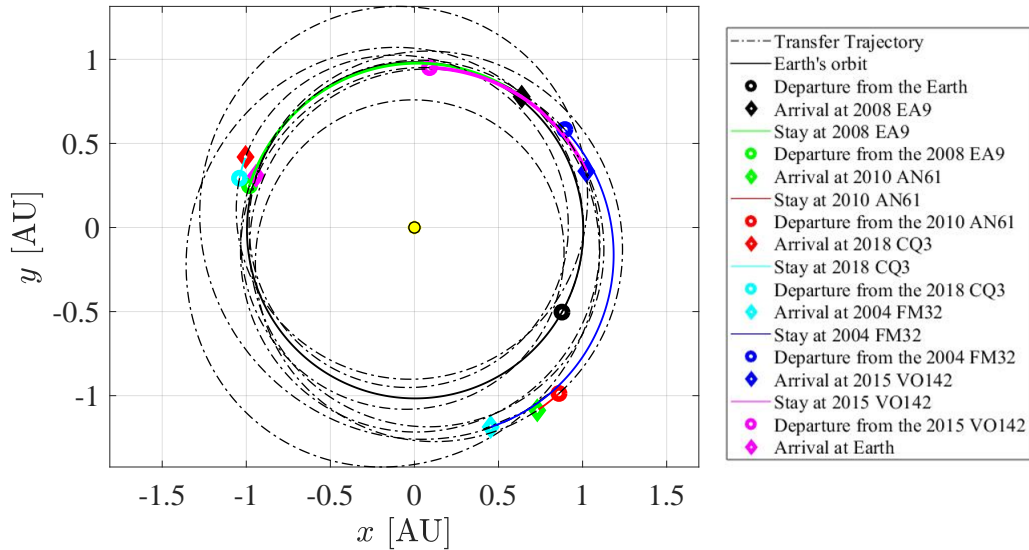


**Figure 9:** Sequence A with no asteroid targeting and  $\alpha = 1$ : heliocentric ecliptic-plane view.

**Table 6:** Mission parameters of the optimized NEA Sequence B. Comparison of optimal results with ANN estimations (in brackets).

Leg	Departure	Arrival	TOF, days	$\Delta V$ , km/s	Stay Time, days
Earth - 2016 TB18	2035/09/13	2036/11/07	421 (444)	2.51 (2.97)	47
2016 TB18 - 1998 KG3	2036/12/24	2038/04/24	486 (456)	9.89 (5.57)	43
1998 KG3 - 162173 Ryugu	2038/06/06	2039/05/27	355 (355)	4.30 (3.97)	65
162173 Ryugu - 2014 UY	2039/07/31	2040/03/23	236 (302)	2.49 (2.70)	28
2014 UY - 2008 EA9	2040/04/20	2041/09/14	512 (532)	4.94 (4.59)	117
2008 EA9 - Earth	2042/01/09	2043/01/26	382 (362)	2.61 (2.73)	—

the propellant mass is used to thrust the spacecraft, its mass  $m$  changes with time as described by the following mass differential equation:

$$\dot{m} = -\frac{T_{max}|\mathbf{N}|}{I_{sp}g_0} \quad (15)$$

where  $I_{sp}$  is the specific impulse of the SEP system.

The OCP is solved by using GPOPS, which uses a discrete non-linear programming (NLP) together with a variable-order adaptive Radau collocation method<sup>37</sup> and the NLP solver IPOPT.<sup>38</sup> The objective of the optimization algorithm is to find the optimal control vector that minimizes the total mass expenditure while fulfilling the dynamics constraints of Eq.(14) at any time. The opti-



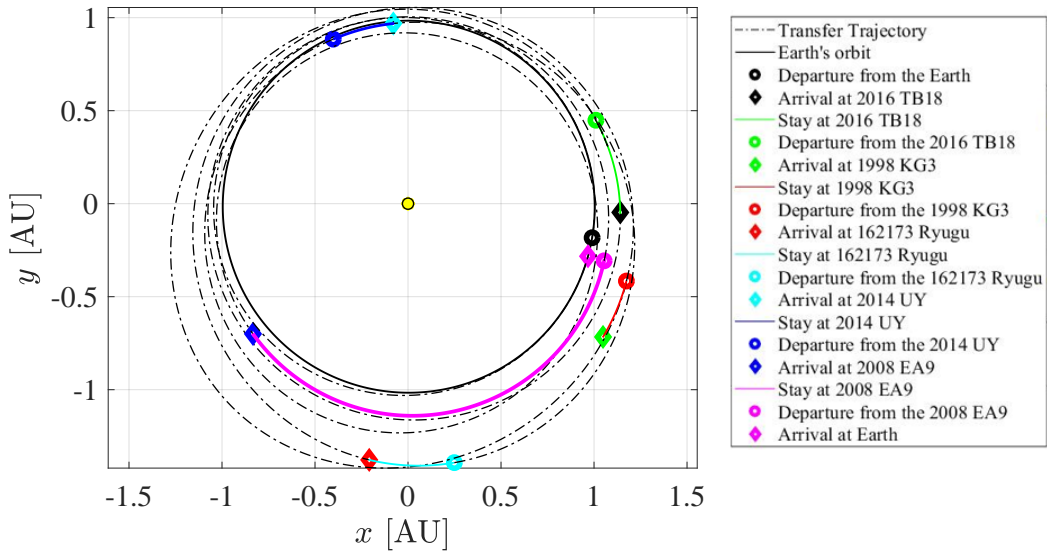


**Figure 10:** Sequence B with target 162173 Ryugu and  $\alpha = 1$ : heliocentric ecliptic-plane view.

**Table 7:** Mission parameters of the optimized NEA Sequence C. Comparison of optimal results with ANN estimations (in brackets).

Leg	Departure	Arrival	TOF, days	$\Delta V$ , km/s	Stay Time, days
Earth - 1998 KG3	2035/09/11	2037/06/09	637 (655)	6.51 (6.81)	86
1998 KG3 - 162173 Ryugu	2037/09/03	2039/01/01	485 (405)	5.31 (4.94)	47
162173 Ryugu - 2017 UY4	2039/02/17	2040/07/24	523 (543)	5.79 (5.90)	98
2017 UY4 - 2000 LY27	2040/10/30	2042/07/23	631 (651)	5.68 (5.17)	120
2000 LY27 - 2001 QC34	2042/11/20	2044/09/12	662 (582)	7.29 (6.49)	109
2001 QC34 - Earth	2044/12/30	2046/01/20	386 (386)	5.87 (5.53)	—

mization is performed on the trajectory leg by leg sequentially, starting from an initial guess which is generated by solving a Lambert problem<sup>39</sup> and using the TOF estimated by the ANN. To allow enough time for close-up observations and/or sample collection a minimum stay time of 20 days is enforced.

Tables 5, 6 and 7 describe the optimized mission characteristics of Sequence A, B and C, respectively. The departure and arrival dates, the TOF, the  $\Delta V$  and stay time are specified for each transfer. To compare the optimized values with those estimated by the ANN, the latter are expressed within brackets. The optimization procedure was able to find a solution for each of the transfers involved, showing that the trajectories are feasible and the spacecraft is able to return to Earth after visiting five asteroids within ten years from departure. The heliocentric ecliptic-plane view of the optimized trajectories for Sequence A, B and C are shown in Fig. 9, 10 and 11.

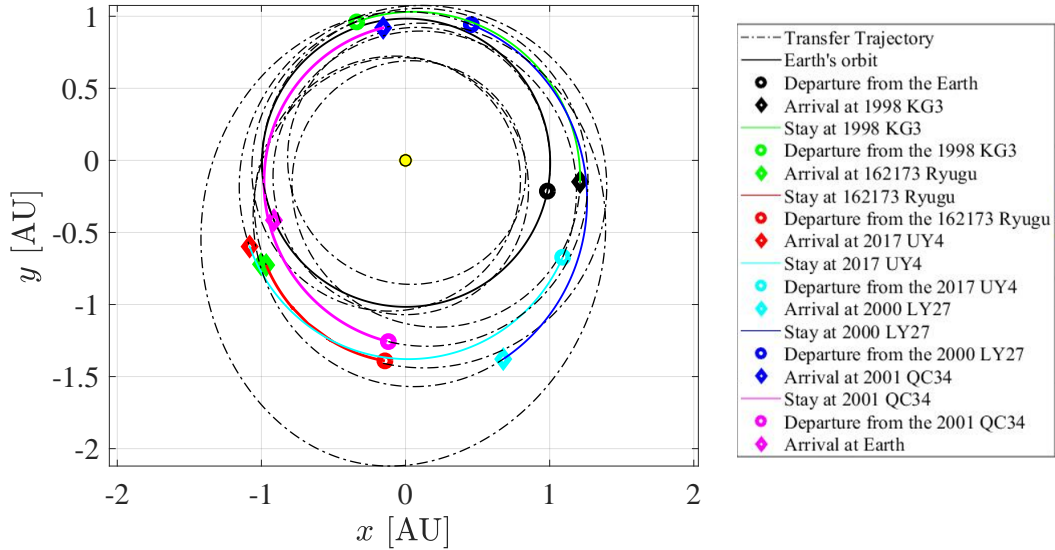


**Figure 11:** Sequence C with no asteroid targeting and  $\alpha = 0.5$ : heliocentric ecliptic-plane view.

The sequence search algorithm generates  $N_S = 200$  asteroid sequences in about 7.6 hours and 3.3 hours for the cases when, respectively, no asteroid or an asteroid is targeted during the search. The simulations have been performed on a machine with a Core i7 processor at 3.4 GHz. In previous works of the authors,<sup>26</sup> the required computational time when an ANN is used in the sequence search has been compared with the time required for other previously used methodologies, which typically required tens of days for a similar simulation to fully compute the multiple NEA sequences. When ANN is used, the algorithm results to be *two* orders of magnitude *faster*.

To evaluate how well the network performs with respect to the optimization procedure, the deviations of the TOF and  $\Delta V$  between the values estimated by the ANN and the optimal ones are calculated as the average percentage errors, i.e.:

$$\mathcal{E}_{TOF} = \frac{1}{N} \sum_{i=1}^N \left( \frac{|TOF_{i,opt} - TOF_{i,ANN}|}{TOF_{i,opt}} \right) \quad (16)$$

$$\mathcal{E}_{\Delta V} = \frac{1}{N} \sum_{i=1}^N \left( \frac{|\Delta V_{i,opt} - \Delta V_{i,ANN}|}{\Delta V_{i,opt}} \right) \quad (17)$$

with  $N$  being the number of legs in the trajectory.

Table 8 presents the percentage errors of three sequences, together with a summary of the total  $\Delta V$  and  $I_V$  for each of them. It can be noted again that, to fly NEA rendezvous missions with greater  $I_V$ , thus visiting asteroids of larger sizes, a larger  $\Delta V$  is generally required which is however still achievable with the chosen propulsion system. The mean error of the Sequences A, B and C is 7.46% for the TOF estimation and 7.27% for the  $\Delta V$  estimation. It can be concluded that the trained network is able to estimate with a reasonably accuracy the cost and duration of transfers from the Earth, between NEAs and back to the Earth, while reducing greatly the computational time.

**Table 8:** Total  $\Delta V$  and  $I_V$  of the selected sequences with the average percentage error between ANN and optimized results.

Sequence	$\Delta V_{tot}$	$I_V$	$\mathcal{E}_{TOF}$	$\mathcal{E}_{\Delta V}$
A (Table 5)	28.11	-135.9	7.87%	6.69%
B (Table 6)	27.35	-119.3	8.12%	8.59%
C (Table 7)	35.75	-103.7	6.40%	6.54%
<b>Mean Error</b>	–	–	<b>7.46%</b>	<b>7.27%</b>

## CONCLUSIONS

An artificial neural network is designed and used to *quickly* estimate the cost and duration of low-thrust, rendezvous transfers between near-Earth asteroids. The network, whose architecture is optimized for this application, is integrated with the sequence search algorithm, which based on a tree-search method, can identify the most convenient sequences from the point of view of the mass expenditure and/or the interest value of the asteroids visited. In this work, an asteroid is considered more *interesting* if it is characterized by a larger size, i.e., lower absolute magnitude and greater interest value,  $I_V$ .

The sequence search algorithm is designed so that, while visiting a defined number of asteroids in a set amount of time, it directs the spacecraft towards asteroids that are closer (in the orbital parameter space) to a target asteroid or, in the final leg, to Earth and eventually transfer to Earth itself. At each leg, the search retains the best 200 sequences in terms of the appealing factor, which derives from the weighted sum of the interest value and  $\Delta V$ . Changing the weight value affects the importance given to  $I_V$  and  $\Delta V$  in the sequence selection process.

The analysis of the distribution of the total  $\Delta V$  and  $I_V$  of the obtained sequences reveals that, when the selection of the sequences during the search is made on the basis of both the  $I_V$  and  $\Delta V$ , more interesting objects can be visited, increasing the overall appeal of the sequences at the cost of a larger  $\Delta V$ . Three sequences were analyzed and fully optimized, to obtain the flight trajectory and control history. It is shown that employing machine learning techniques within the sequence search algorithm greatly reduces the computational time, while still ensuring a high accuracy with an average percentage error of about 7% with respect to the optimal values.

## ACKNOWLEDGMENTS

Giulia Viavattene gratefully acknowledges the support received for this research from the James Watt School of Engineering at the University of Glasgow for funding the research under the James Watt sponsorship program.

## REFERENCES

- [1] A. Chaikin, *A Man On the Moon: The Voyages of the Apollo Astronauts*. New York: Penguin Books, 3rd ed., 2007.
- [2] D. Lauretta, “OSIRIS-REx Asteroid Sample-Return Mission,” *Handbook of Cosmic Hazards and Planetary Defense*, 2015, pp. 543–567, 10.1007/978-3-319-03952-744.
- [3] J. J. Lissauer, and I. de Parter, *Fundamental Planetary Science*. Cambridge University Press, 2013.

- [4] J. T. Grundmann, W. Bauer, R. C. Boden, M. Ceriotti, F. Cordero, B. Dachwald, E. Dumont, C. D. Grimm, D. Herčik, A. Hérique, T. Ho, R. Jahnke, W. Kofman, C. Lange, R. Lichtenheldt, C. McInnes, T. Mikschl, E. Mikulz, S. Montenegro, I. Moore, I. Pelivan, A. Peloni, D. Plettemeier, D. Quantius, S. Reershemius, T. Renger, J. Riemann, Y. Rogez, M. Ruffer, K. Sasaki, N. Schmitz, W. Seboldt, P. Seefeldt, P. Spietz, T. Sprowitz, M. Sznajder, N. Tóth, G. Viavattene, E. Wejmo, C. Wiedemann, F. Wolff, and C. Ziach, “Responsive exploration and asteroid characterization through integrated solar sail and lander development using small spacecraft technologies,” *6th IAA Planetary Defense Conference, Washington DC, USA*, 2019.
- [5] A. Hérique, B. Agnus, E. I. Asphaug, M. A. Barucci, P. Beck, J. Bellerose, J. Biele, L. Bonal, P. Bousquet, L. Bruzzone, et al., “Direct Observations of Asteroid Interior and Regolith Structure: Science Measurement Requirements.” *Advances in Space Research, Elsevier*, Vol. 62, No. 8, 2018, pp. 2141–2162, 10.1016/j.asr.2017.10.020.
- [6] D. Agnolon, “Study Overview of the Near Earth Asteroid Sample Return,” tech. rep., ESTEC, ESA, Noordwijk, The Netherlands, 2007.
- [7] M. Vergaaij, C. McInnes, and M. Ceriotti, “Economic assessment of high-thrust and solar-sail propulsion for near-earth asteroid mining,” *Advances in Space Research, Elsevier*, 2020, 10.1016/j.asr.2020.06.012.
- [8] M. Yoshikawa, J. Kawaguchi, and A. Fujiwara, “Hayabusa Sample Return Mission,” *Asteroids IV*, 2015, pp. 397–418, 10.2458/azu-uapress-9780816532131-ch021.
- [9] Y. Tsuda, M. Yoshikawa, M. Abe, M., H. Minamino, and S. Nakazawa, “System design of the Hayabusa 2: Asteroid sample return mission to 1999 JU3,” *Acta Astronautica*, Vol. 91, 2013, pp. 356–362, 10.1016/j.actaastro.2013.06.028.
- [10] C. R. McInnes, *Solar Sailing - Technology, Dynamics and Mission Applications*. 1999, 10.1007/978-1-4471-3992-8.
- [11] A. Mereta and D. Izzo, “Target selection for a small low-thrust mission to near-Earth asteroids,” *Astrodynamics*, Vol. 2, No. 3, 2018, pp. 249–263.
- [12] D. Izzo, L. F. Simoes, C. H. Yam, F. Biscani, D. Di Lorenzo, A. Bernardetta, and A. Cassioli, “GTOC5 : Results from the European Space Agency and University of Florence,” *Acta Futura*, Vol. 8, No. November, 2014, pp. 45–56, 10.2420/AF08.2014.45.
- [13] J. R. Wertz, *Orbit & Constellation Design & Management*. New York: Springer, 2009.
- [14] R. G. Jahn, *Physics of Electric Propulsion*. New York: McGraw-Hill Book Company, 2006.
- [15] H. Yang, G. Tang, and F. Jiang, “Optimization of observing sequence based on nominal trajectories of symmetric observing configuration,” *Astrodynamics*, Vol. 2, No. 1, 2018, pp. 25–37, 10.1007/S42064-017-0009-2.
- [16] H. Li, S. Chen, D. Izzo, and H. Baoyin, “Deep Networks as Approximators of Optimal Transfers Solutions in Multitarget Missions,” *Acta Astronautica*, 2019, 10.1016/j.actaastro.2019.09.023.
- [17] A. Peloni, M. Ceriotti, and B. Dachwald, “Solar-Sail Trajectory Design for a Multiple Near-Earth-Asteroid Rendezvous Mission,” *Journal of Guidance, Control, and Dynamics*, Vol. 39, sep 2016, pp. 2712–2724, 10.2514/1.G000470.
- [18] G. Tang, F. Jiang, and J. Li, “Trajectory Optimization for Low-Thrust Multiple Asteroids Rendezvous Mission,” *AIAA/AAS Astrodynamics Specialist Conference*, 2015, 10.1515/jnum-2014-0003.
- [19] M. Di Carlo, J. M. R. Martin, N. Gomez, and M. Vasile, “Optimised Low-Thrust Mission to the Atira Asteroids,” *Advances in Space Research*, Vol. 59, 2017, pp. 1724–1739, 10.1016/j.asr.2017.01.009.
- [20] B. Dachwald, “Optimization of Interplanetary Solar Sailcraft Trajectories,” *Journal of Guidance, Control, and Dynamics*, Vol. 27, No. 1, 2004, 10.2514/1.9286.
- [21] D. Hennes, D. Izzo, and D. Landau, “Fast Approximators for Optimal Low-Thrust Hops Between Main Belt Asteroids,” *IEEE Symposium Series on Computational Intelligence (SSCI)*, 2016, 10.1109/SSCI.2016.7850107.
- [22] A. Mereta, D. Izzo, and A. Wittig, “Machine Learning of Optimal Low-Thrust Transfers Between Near-Earth Objects,” *Hybrid Artificial Intelligent Systems*, 2017, pp. 543–553, 10.1007/978-3-319-59650-146.
- [23] C. Sánchez-Sánchez and D. Izzo, “Real-time optimal control via Deep Neural Networks: study on landing problems,” *Journal of Guidance, Control, and Dynamics*, Vol. 41, No. 3, 2018, pp. 1122–1135, 10.1023/B:CJOP.0000010527.13037.22.
- [24] H. Peng and X. Bai, “Artificial Neural Network–Based Machine Learning Approach to Improve Orbit Prediction Accuracy,” *AIAA Journal of Spacecraft and Rockets*, Vol. 55, No. 5, 2018, pp. 1–13, 10.2514/1.A34171.

- [25] Y. Song and S. Gong, "Solar-Sail Trajectory Design of Multiple Near Earth Asteroids Exploration Based on Deep Neural Network," *Aerospace Science and Technology*, Vol. 91, 2019, pp. 28–40, 10.1016/j.ast.2019.04.056.
- [26] G. Viavattene and M. Ceriotti, "Artificial Neural Network for Preliminary Multiple NEA Rendezvous Mission Using Low Thrust," *70th International Astronautical Congress (IAC), Washington DC, USA*, 2019.
- [27] L. Rutkowski, M. Korytkowski, R. Scherer, R. Tadeusiewicz, L. A. Zadeh, and J. M. Zurada, *Artificial Intelligence and Soft Computing*. Zakopane, Poland: Springer, 2013, 10.1007/978-3-642-38658-9.
- [28] I. Goodfellow, Y. Bengio, and A. Courville, *Deep Learning*. Cambridge, Massachusetts: The MIT Press, 2016.
- [29] R. Rojas, *Neural Networks: A Systemic Introduction*. New York: Springer, 1996, 10.1016/0893-6080(94)90051-5.
- [30] W. Wiesel, *Spaceflight Dynamics: Third Edition*. Cambridge, Massachusetts: CreateSpace, 2017.
- [31] P. De Pascale and M. Vasile, "Preliminary Design of Low-Thrust Multiple Gravity-Assist Trajectories," *AIAA Journal of Spacecraft and Rockets*, Vol. 43, No. 5, 2006, pp. 1065–1076, 10.2514/1.19646.
- [32] F. Vilas, "Spectral characteristics of Hayabusa 2 near-Earth asteroid targets 162173 1999 JU3 AND 2001 QC34," *The Astronomical Journal*, Vol. 135, 2008, pp. 1101–1105, 10.1088/0004-6256/135/4/1101.
- [33] D. J. Tholen and M. A. Barucci, "Asteroid taxonomy," *Asteroids II, Proceedings of the Conference*, No. March, 1989, pp. 298–315.
- [34] A. W. Harris and A. W. Harris, "On the Revision of Radiometric Albedos and Diameters of Asteroids," *Icarus*, Vol. 126, No. 2, 1997, pp. 450–454, 10.1006/icar.1996.5664.
- [35] S. R. Chesley, P. W. Chodas, A. Milani, G. B. Valsecchi, and D. K. Yeomans, "Quantifying the Risk Posed by Potential Earth Impacts," *Icarus*, Vol. 159, No. 2, 2002, pp. 423–432, 10.1006/icar.2002.6910.
- [36] J. T. Betts, *Practical Methods for Optimal Control and Estimation Using Nonlinear Programming*. Philadelphia: SIAM Press, second ed., 2010.
- [37] M. A. Patterson and A. V. Rao, "GPOPS-II: A MATLAB Software for Solving Multiple-Phase Optimal Control Problems using hp-Adaptive Gaussian Quadrature Collocation Methods and Sparse Nonlinear Programming," *ACM Transactions on Mathematical Software*, Vol. 41, No. 1, 2014, 10.1145/2558904.
- [38] A. Wachter and L. T. Biegler, "On the Implementation of an Interior-Point Filter Line-search Algorithm for Large-scale Non-linear Programming," *Mathematical Programming*, Vol. 106, No. 1, 2006, pp. 25–57, 10.1007/s10107-004-0559-y.
- [39] H. Curtis, *Orbital Mechanics for Engineering Students*. Elsevier, 2005.